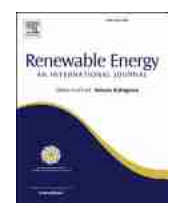


Contents lists available at ScienceDirect

Renewable Energy

journal homepage: www.elsevier.com/locate/renene



Increased ground temperatures in urban areas: Estimation of the technical geothermal potential



Jaime A. Rivera ^{a, *}, Philipp Blum ^b, Peter Bayer ^c

- ^a ETH Zürich, Department of Earth Sciences, Sonneggstrasse 5, 8092 Zurich, Switzerland
- b Karlsruhe Institute of Technology (KIT), Institute for Applied Geosciences (AGW), Kaiserstraße 12, 76131 Karlsruhe, Germany
- ^c Ingolstadt University of Applied Sciences, Ingolstadt, Germany

ARTICLE INFO

Article history:
Received 5 April 2016
Received in revised form
21 October 2016
Accepted 2 November 2016
Available online 3 November 2016

Keywords:
Geothermal energy
Low-enthalpy
Heat transport
Technical potential
Subsurface urban heat island

ABSTRACT

Many cities leave a considerable thermal footprint in the subsurface. This is caused mainly by accelerated heat fluxes from warmed basements, pavements and buried infrastructures. Even though rough estimations of the theoretical heat content in urban ground exist, there is no insight available on the technical potential of such subsurface urban heat islands. By considering borehole heat exchangers (BHEs) for geothermal exploitation, new opportunities arise for planning sustainable systems within cities through utilization of accelerated ground heat input from urban structures. This is feasible at moderate heat extraction rates even without any active (seasonal) recharging of the BHEs. For typical conditions in central Europe and a given system's life time, each additional degree of urban ground heating could save around 4 m of the borehole length for the same heating power supply. We inspect implications for a single BHE as well as complete coverage of cities, which is approximated by an infinite field of BHEs. The results show that shallower systems favour renewable operation, and urban technical potential of geothermal use increases by up to 40% when compared to rural conditions.

© 2016 Elsevier Ltd. All rights reserved.

1. Introduction

The shallow ground is considered as a large energy reservoir, and the thermal capacity of low-enthalpy geothermal installations shows global growth rates of around 7% at present [1]. Most common devices are borehole heat exchangers (BHEs), where a heat carrier fluid exchanges heat with the ambient ground by circulation in vertical boreholes. Although much more energy is stored in the ground than is used, local geothermal energy availability might be limited. Especially in areas with dense populations and high installed capacities, competition for the ground is high [2–4]. In Switzerland, for example, with the highest density of BHEs worldwide, local authorities caution overexploitation of the ground [5].

Previous works implemented GIS-based models to estimate the spatially distributed geothermal potential in specific regions or cities ([6-12]). Common to these regional models is that they consider the variability of the thermal properties of the subsurface and expected heat extraction rates, which are specified by

* Corresponding author.

E-mail address: jaime.rivera@erdw.ethz.ch (J.A. Rivera).

guidelines such as the German VDI [13]. Schiel et al. [7], for instance, applied this to the city of Ludwigsburg, Germany. They compared the spatially distributed heating demands and the energy supplied by BHEs fields. In the same manner, Zhang et al. [14] estimated the spatial variability of the capacity and electricity consumption for different BHEs distributions in the city of Westminster, London. Both studies reveal how the specific heating demands may be fully or partially supplied by multiple BHEs, employing assumptions and simplifications that restrict the model.

One common simplification is related to the way these models account for urban heat sources such as heat losses from basements, underground infrastructure (e.g., tunnels, district heating and sewage networks) and heat input from increased ground surface temperature [15–19]. Generally, these influences exhibit a high variability in space and time that is commonly neglected in GIS-supported models. Depending on their strength and timing, these man-induced thermal alterations can significantly change the ground temperature down to several tens of meters in the subsurface [20]. Bayer et al. [21], for instance, employed analytical models to estimate the relative contribution of climate forcing and urban sources such as paved areas and buildings to urban ground. For this, four measured temperature-depth-profiles (TDPs) taken in areas with different degrees of urbanization in the city and suburbs

Nomenclature		x, y, z coordinates where temperature is evaluated (m)				
		$x_a, x_{b_i} y$	y_a , y_b boundary coordinates of the specific land use (m)			
а	thermal diffusivity ($m^2 s^{-1}$)					
В	separation of BHEs (m)	Greek s	ymbols			
F_o	Fourier number	λ	thermal conductivity of porous medium (W m^{-1} K $^{-1}$)			
g	g-function	τ	time at which a heat pulse is released (s)			
Н	borehole length (m)	θ	dimensionless temperature			
k	geothermal gradient (°C m ⁻¹)					
q	heat flow rate per unit length (W m^{-1})	Abbrevi	iations			
Q_T	dimensionless number	BHE	borehole heat exchanger			
r_b	borehole radius (m)	BW	borehole wall			
R	transient total thermal resistance (m K W^{-1})	FLS	finite line source			
R_b	effective thermal resistance of the borehole (m K W^{-1})	GIS	geographical information system			
t	time (s)	GST	ground surface temperature			
t_s	characteristic time (s)	IC	initial conditions			
t_{urb}	time of preexisting urban warming before BHE	MFLS	moving finite line source			
	operation (s)	SIA	Schweizerischer Ingenieur-und Architektenverein			
T	temperature in the porous medium (°C)	SUHI	subsurface urban heat island			
T_{BHE}	temperature change induced by BHE operation (°C)	TBC	top boundary condition			
T_{BW}	temperature at the borehole wall (°C)	TDP	temperature depth profile			
T_{FLS}	temperature associated with the FLS solution (°C)	VDI	Verein Deutscher Ingenieure			
ΔT_{GST}	net increased temperature at the ground surface (°C)					
T_k	unaffected ground surface temperature (°C)	Conven	tions			
T_{IC}	temperature associated with the IC solution (°C)	\overline{X}	depth-averaged value of the quantity X			
T_{TBC}	temperature associated with the TBC solution (°C)					

of Zurich were inspected. It was demonstrated that urban structures are responsible for at least 50% of the additional energy stored in the subsurface. This is consistent with earlier work on other central European cities, which reveal large thermal anomalies in the upper urban ground, known as subsurface urban heat islands (SUHIs). These indicate accelerated heat flux from the basements of buildings and paved ground as the main drivers [22-24]. Zhu et al. [25] compared the additional energy stored in urban ground with the annual heating demand in several cities to calculate the geothermal potential of SUHIs. They focused on the total anthropogenic heat accumulated beneath cities (theoretical geothermal potential), However, the practically extractable energy (technical potential) of the urban subsurface is not addressed [26]. The present work intends to provide this. The objective here is the estimation of the increased technical potential of the shallow urban ground, which could be exploited by vertical ground source heat pump (GSHP) systems equipped with BHEs. As in previous GISbased approaches, groundwater effects are neglected.

Various analytical and numerical approaches exist for simulating BHEs [27–30]. Among these, the unitary response factor approach based on g-functions [31,32] is widely employed. In a BHE, the circulating fluid exchanges heat with the ground through conduction. The g-functions yield the relationship between the mean borehole wall temperature and the heat extraction rate [33,34].

The *g*-functions are formulated depending on the boundary conditions at the borehole wall [35,36]. In the original formulation, uniform temperature was assumed, requiring an expensive and less flexible numerical solution. To improve this, analytical finite line source (FLS) models were explored [37–41]. FLS models have been proven as acceptable approximation, especially in the case of single BHEs and extended time scales [33,42,43]. Within the scope of this study, the FLS-based *g*-function is convenient for two main reasons. First, high-frequency signals of the heat extraction rate are not relevant here, because the focus is set on the long term performance of the BHE and the role of land-surface effects (rather than

the BHE design itself). Second and more importantly, the FLS model enables the superposition of existing analytical expressions to account for increased ground surface temperatures. Consequently, this work presents a fast and analytical framework that incorporates the time-dependent interaction between the natural geothermal reservoir, urban land surface effects and technological use. Moreover, the analytical formulation facilitates direct implementation within GIS-based models as the ones described above.

In the following, we first present the modified formulation of the mean borehole wall temperature that incorporates the dynamics induced by increased ground surface temperatures (GSTs). This formulation enables the analysis of different operation schemes, including renewability criteria. The analysis is carried out for two extremes: for a single installation and for an infinite field, rendering a massive exploitation at the city scale. As a result, the technical potential of BHEs in cities with SUHIs is motivated and the methodology is demonstrated for an example case in the city of Zurich, Switzerland.

2. Methodology

2.1. Model description

We consider the urban subsurface as a semi-infinite space with thermal conductivity λ and thermal diffusivity a. In this space, BHEs are represented by line sources and the increased ground surface temperature (GST) by continuous doublets distributed over the top boundary [44,45]. The thermal changes induced by these modeling entities, together with the initial thermal conditions, determine the temperature at any point and time. Of special interest is the temperature at the borehole wall T_{BW} since it influences the heat extraction rate q from the BHE [31]. This temperature can be obtained by superposing the thermal changes induced by the interacting sources. For this, the heat conduction problem should be solved for its homogeneous and non-homogenous boundary value components [46,47]. On the one hand, the homogeneous boundary

value problem considers that the temperature at the top boundary is zero (no increased GST). Thus, the borehole wall temperature is only driven by the thermal changes induced by BHE operation, T_{BHE} . For these conditions, the g-function g relates the mean borehole wall temperature $\overline{T_{BW}}$ and the heat extraction rate q [31]:

$$\overline{T_{BW}(t)} = \overline{T_{BHE}(t)} = \frac{q}{2\pi\lambda} g\left(\frac{t}{t_s}, \frac{r_b}{H}\right) \tag{1}$$

where t is the time, $t_s = H^2/9a$ is a characteristic time, H is the borehole length and r_b is the borehole radius. In the original formulation by Eskilson [31], the g-function is numerically evaluated for a specific system configuration. Alternatively, by calculating the mean borehole wall temperature with the FLS model, the following semi-analytical expression is obtained ([33,38]):

$$\overline{T_{BHE}(t)} = \overline{T_{FLS}(t)} = \frac{q}{8\lambda\pi} \int_{\frac{r_b^2}{4at}}^{\infty} \frac{1}{\phi} \exp(-\phi) \left\{ 4erf\left(\frac{H\sqrt{\phi}}{r_b}\right) - 2erf\left(\frac{2H\sqrt{\phi}}{r_b}\right) + \frac{r_b}{H\sqrt{\pi\phi}} \left[4\exp\left(-\frac{H^2\phi}{r_b^2}\right) - \exp\left(-\frac{4H^2\phi}{r_b^2}\right) - 3 \right] \right\} d\phi$$
(2)

On the other hand, if the temperature at the ground surface is not zero, the solution of the nonhomogeneous boundary value problem T_{TBC} should be superposed to T_{BHE} , as verified by Rivera et al. [44,45] for urban land surface effects. It was also implemented by Bandos et al. [38] for estimating the influence of ambient temperature in thermal response tests, and by Duan and Naterer [48] for estimating the temperature beneath power transmission towers.

The mean borehole wall temperature is obtained by averaging the superposed solutions over the depth H as follows:

$$\overline{T_{BW}(t)} = \overline{T_{BHE}(t)} + \overline{T_{TBC}(t)} + \overline{T_{IC}}$$
(3)

where T_{IC} refers to the initial or undisturbed temperature. If this temperature is roughly approximated by a geothermal gradient k, and surface temperature T_k , the associated mean temperature along the length H is $\overline{T_{IC}} = T_k + kH/2$. In the original g-function, the temperature T_{BHE} is computed for a constant background temperature [49]. In contrast, this work considers the transient effect of the increased GST (e.g. T_{TBC}) on the long term evolution of the borehole wall temperature and associated heat extraction rates. To provide the T_{TBC} solution, it is necessary to consider the spatial variability of land use in cities. For this, the solution provided by Rivera et al. [44] can be formulated for selected urban areas with specified land use. These formulations are then superimposed to the global solution (application examples are shown in Refs. [44,50,51]). Here, it is assumed that each land use scenario can be characterized by its own constant or time dependent increased ground surface temperature, $\Delta T_{GST}(t)$ [21,52]. The depth-averaging of this solution over the length *H* yields:

$$\begin{split} \overline{T_{TBC}(x,y,t)} &= \frac{1}{8\sqrt{\pi}} \int\limits_{\frac{H^2}{4at}}^{\infty} \Delta T_{GST} \left(t - \frac{H^2}{4a\phi} \right) \left[\frac{1 - \exp(\phi)}{\phi^{3/2}} \right] \\ &\times \left[erf\left(\frac{y - y_b}{H} \sqrt{\phi} \right) - erf\left(\frac{y - y_a}{H} \sqrt{\phi} \right) \right] \\ &\times \left[erf\left(\frac{x - x_b}{H} \sqrt{\phi} \right) - erf\left(\frac{x - x_a}{H} \sqrt{\phi} \right) \right] d\phi \end{split} \tag{4}$$

where x, y are the coordinates of the evaluation point in the horizontal plane and y_a , y_b , x_a , x_b are the coordinates of the specific land use area with temperature $\Delta T_{GST}(t-H^2/(4a\varphi))$.

Initially, for the purpose of generality, it is assumed that the spatially variable GST can be represented by a mean constant value, ΔT_{GST} . For a specific location, with given land use distribution, this value could be an area-weighted GST that renders the mean annual ground surface temperature. According to this, the land use effect is represented by an infinite plane that induces a transient vertical heat flux into the ground. An analytical expression for this effect can be derived from the solutions presented in Refs. [38,46], which after being averaged over the reference length H, reads:

$$\overline{T_{TBC}(t)} = \frac{1}{H} \int_{0}^{H} \left[\frac{z}{2\sqrt{\pi a}} \int_{0}^{t} \frac{\Delta T_{GST}}{(t-\tau)^{3/2}} exp\left(-\frac{z^{2}}{4a(t-\tau)}\right) d\tau \right] dz$$

$$= \Delta T_{GST} \left\{ erf\left(-\frac{H}{\sqrt{4at}}\right) + \sqrt{\frac{4at}{\pi H^{2}}} \left[1 - \exp\left(-\frac{H^{2}}{4at}\right)\right] + 1 \right\}$$

$$= \Delta T_{GST} \cdot f\left(F_{o} = \frac{at}{H^{2}}\right)$$
(5)

where F_0 is the Fourier number. To accurately superpose $\overline{T_{TBC}(t)}$ to $\overline{T_{IC}}$ in Eq. (3), ΔT_{GST} represents the excess in ground surface temperature above T_k . This means that the absolute urban ground surface temperature is $T_k + \Delta T_{GST}$. In Eq. (2) and Eq. (5), the time is specified by the same variable t. This means that both processes, increased GST and BHE operation, start at the same time. However, a time lag between those processes may exist. In city centers for instance, the thermal forcing associated with land use changes had been acting for several decades before the installation of any BHE. If this time lag is t_{urb} and the BHE starts operation at t=0 then the time in Eq. (5) should be $t_{urb}+t$.

Taking the original g-function as a reference, it is necessary to obtain a dimensionless form of Eq. (3) to generally describe the effect of elevated ground surface temperature. This dimensionless form can be derived as follows:

$$\left[\overline{T_{BW}\left(\frac{t}{t_{s}}\right)} - \overline{T_{IC}}\right] \frac{2\pi\lambda}{q} = \overline{\theta_{BW}\left(\frac{t}{t_{s}}\right)} = g\left(\frac{t}{t_{s}}, \frac{r_{b}}{H}\right) \\
+ 2\pi \frac{\lambda\Delta T_{CST}}{q} f\left(\frac{t_{urb} + t}{t_{s}}\right) = g\left(\frac{t}{t_{s}}, \frac{r_{b}}{H}\right) \\
+ 2\pi Q_{T} f\left(\frac{t_{urb} + t}{t_{s}}\right) \tag{6}$$

where the dimensionless number $Q_T = \lambda \Delta T_{GST}/q$, compares the strength of the surficial forcing ΔT_{GST} , to the heat extraction rate q, of the BHE.

According to Eq. (6), urban land surface effects increase the mean borehole wall temperature and allow a higher extraction rate q. By comparing these affected rates with those ones obtained under undisturbed conditions, the increased technical geothermal potential is estimated. For this, different system configurations and exploitation scenarios will be analysed.

At this point, it is worth to discuss some assumptions in the model that suggest a limited scope of applicability at first glance. One is the assumption of a homogenous porous medium. However, for conduction dominated conditions, using average or effective thermal properties (homogenization), has proven to be a good approximation [32,49]. Another constraining assumption is the omission of groundwater flow in the model. On the one hand,

several studies have demonstrated that thermally unaffected groundwater flow enhances the performance of GSHP systems (e.g. [53,54]). On the other hand, significant groundwater flow close to the ground surface also promotes higher heat losses from surficial sources [55]. Preliminary analysis implementing the moving finite line source (MFLS [56]), indicates that a rather low effective thermal velocity easily overprints any ground surface temperature effects on the mean borehole wall temperature. In these cases, (thermally) undisturbed groundwater flow shapes the thermal plumes without changing significantly the overall energy balance [57,58]. A few studies have been carried out in urban areas significantly influenced by dynamic aquifers where the presented analytical models have limited applicability. These studies necessarily rely on measurements and numerical simulations of the interaction of these aguifers and near-surface urban sources [59-62].

2.2. Scenarios of analysis

There are diverse standards for BHE installation and planning in different countries [63] that typically restrict induced ground temperature variations, heat extraction rates and/or the lifetime of the geothermal system. This work considers the regulations for planning and construction provided by the Swiss Society of Engineers and Architects (SIA). Specifically, its norm 384/6 defines the lowest allowed temperature in the circulating fluid of ground coupled heat pumps. According to the norm, the mean fluid temperature should not be lower than -1.5~°C after 50 years of operation [64]. If this mean fluid temperature is $\overline{T_{fluid}}$, then it is possible to relate this temperature and Eq. (3) as follows [32]:

$$\overline{T_{fluid}} = \overline{T_{TBC}(t_{urb} + t)} + \overline{T_{IC}} + qR(t) = \overline{T_{BW}(t)} + qR_b$$
 (7)

where the sum $\overline{T_{TBC}(t_{urb}+t)}+\overline{T_{IC}}$ is usually referred to as the undisturbed ground temperature, R(t) is the transient total thermal resistance and R_b is the effective thermal resistance of the borehole. For an unbalanced extraction rate q, $\overline{T_{BHE}(t)}+qR_b$ acts against the background temperature provided by $\overline{T_{TBC}(t_{urb}+t)}+\overline{T_{IC}}$.

Two scenarios are discussed in the following:

- The "depleting scenario", which corresponds to a finite operation period of 50 years.
- The "renewable scenario", which corresponds to an infinite operation period, where the heat extraction rate is balanced by natural sources [3,65].

Results for both scenarios are discussed along with their corresponding 'base case', which refers to the undisturbed conditions. In this way, the net energy gain is associated with urban effects, and thus the related technical potential can be quantified and discussed.

The analyses are carried out for a reference site, specified by the parameters listed in Table 1. The given values of the geothermal gradient, the thermal diffusivity and the thermal conductivity are representative for the city of Zurich [21] and are characteristic for unconsolidated sediments typically found beneath many central European cities [66]. The magnitude of R_b is within the expected range of values for long term BHE operation [49]. Finally, the value for T_k is site specific and corresponds to the estimations for the city of Zurich described in [21].

For the following analysis, a range of borehole lengths (*H*) between 50 m and 200 m is considered. The upper limit is chosen based on observed urban temperature-depth-profiles (TDPs) that typically show thermal anomalies reaching up to 150 m depth [17,20]. Moreover, the upper limit of 200 m minimizes the effect of

Table 1 Parameters for the reference site taken from Refs. [21,66].

Parameter	Value
Thermal diffusivity, $a (m^2 s^{-1})$	1×10^{-6}
Thermal conductivity, λ (W m ⁻¹ K ⁻¹)	2.5
Borehole radius, r_b (m)	0.1
Effective borehole thermal resistance, R_b (W ⁻¹ m K)	0.15
Background surface temperature, T_k (°C)	10
Vertical geothermal gradient, k (°C m ⁻¹)	0.03

inaccuracies in the analytical model related to the assumption of an uniform heat extraction rate along the depth [67]. This assumption may be critical for deeper applications because with higher ground temperatures (due to the geothermal gradient) it is expected that heat extraction rates also increase with depth. Finally, for specification of increased urban ground-surface temperature, ΔT_{CST} , a range of 0.5–5 K is chosen according to the findings in [22,23].

3. Results and discussion

3.1. Single BHE

3.1.1. Effect of land surface forcing on mean borehole wall temperature

The dimensionless mean borehole wall temperature $(\overline{\theta_{BW}})$ is crucial for estimating the technical geothermal potential, and it is scrutinized first, Fig. 1a shows the influence of increasing groundsurface warming (expressed by Q_T), assuming that urban ground heating and BHE operation start simultaneously ($t_{urb} = 0$). The curve $Q_T = 0$ corresponds to the original g-function without the transient effect induced by ΔT_{GST} . In this case, the sustained drop in $\overline{\theta_{BW}}$ is due to the continuous heat extraction q. For $\Delta T_{GST} > 0$, the quantity $Q_T = \lambda \Delta T_{GST}/q$ increases proportionally to its magnitude. The associated curves depicted in Fig. 1a exhibit a characteristic minimum in $\overline{\theta_{BW}}$. The time at which this minimum occurs indicates the instant when GST effects balance the temperature drop induced by q such that the heat flux from the surface compensates the heat extraction. At later times, continuously high ground-heat flux replenishes the cooled ground. Pronounced ΔT_{GST} is associated with a higher mean borehole wall temperature.

Fig. 1b examines the same conditions as in Fig. 1a, but assumes that urbanization has started 100 years ago ($t_{urb}=100$ years). In this case, a subsurface urban heat island (SUHI) pre-exists before the BHE operation. The influence of increased ground-surface temperatures as expressed by Q_T is clearly enhanced, especially at early operation times. This is a consequence of the linear superposition of the different solutions indicated in Eq. (3). For a given borehole length H, there is a time when SUHI covers this depth and the changes in the mean borehole wall temperature start to diminish. If the operation time of the BHE is several times longer than this characteristic time, then at the end of the time window, $\overline{\theta_{BW}}$ becomes insensitive to t_{urb} (Fig. 1b).

The described temporal dynamics of the mean borehole wall temperature can be transferred to the mean fluid temperature $\overline{T_{fluid}}$ via Eq. (7). In this way, it is possible to estimate the heat extraction rates that fulfil the conditions of the depleting and renewable scenarios as discussed in the following.

3.1.2. Depleting scenario

The depleting scenario assumes that the reservoir is exhausted after 50 years of operation. For this condition, Fig. 2 depicts the technical geothermal potential for different timings and intensities of surface warming.

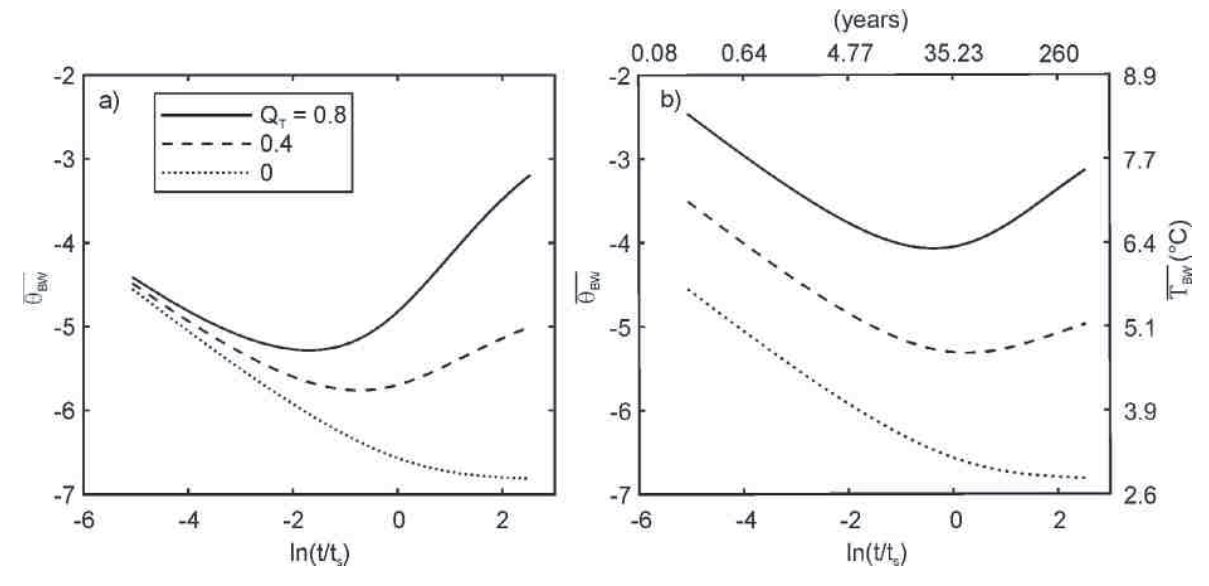


Fig. 1. Dimensionless mean borehole wall temperature over dimensionless time: a) $t_{urb} = 0$ years and b) $t_{urb} = 100$ years (the magnitudes in °C and years correspond to the parameters shown in Table 1 with q = 20 W m⁻¹ and H = 100 m). A higher Q_T indicates a stronger effect from ΔT_{GST} relative to the heat extraction rate q. $Q_T = 0$ is the original g-function neglecting urbanization effects.

Fig. 2a shows the heat extraction rates for $t_{urb}=0$ and 100 years. These rates are mean annual values and are of the same magnitude as those discussed in [7,49,68]. While these rates have values between 26 and 27 W m⁻¹ for the lowest assumed ground surface warming ($\Delta T_{GST}=0.5$ K), they reach values higher than 30 W m⁻¹ at the upper limit of $\Delta T_{GST}=5$ K. Clearly, the rates are more sensitive to ΔT_{GST} for the shallower BHEs.

The characteristic curvature is the result of the complementary effect between the initial thermal conditions given by the geothermal gradient and the increased GST on top. For a given isorate curve q, there is a length H^* above and below which the extraction rate q can be kept at lower ΔT_{GST} . For a BHE with $H > H^*$, the natural geothermal gradient dominates and thus, the rate q is sustained by decreasing ΔT_{GST} .

For any selected point in the domain of Fig. 2a, the extraction rates are higher for $t_{urb}=100$ years than for $t_{urb}=0$ years. For better insight, the ratio of the rates q ($t_{urb}=100$ years)/q ($t_{urb}=0$ years) is depicted in Fig. 2b. It is shown that the gain in q due to 100 years of urbanization ranges between 1% and 6%. The minimum ΔT_{GST} for a given curve is an indicator for the penetration depth of ΔT_{GST} in the 100 years period. Taking for example $\Delta T_{GST}=3$ K, the maximum relative gain from this preexisting GST is obtained for a BHE with borehole length of $H\approx 112$ m.

Fig. 2c indicates the total power extracted from a single BHE. The power is mainly controlled by H. However, for a given power, elevated ground surface temperature tends to decrease the required BHE length at an approximate rate of 4.5 m for 1 K. For a 2 kW demand (annually averaged) and assuming $\Delta T_{GST} = 0.5$ K, for instance, a BHE has to be drilled 80 m. This is reduced to 60 m given a value of $\Delta T_{GST} = 5$ K. Note that in practice, planning of appropriate BHE configuration also has to consider high frequencies in the energy demand (daily and hourly loads), which may appreciably increase the required length [69]. These results imply that an optimized use of the stored energy in urban areas can be achieved by combining more shallow BHEs to supply the base demand and fewer deep exchangers for buffering peak loads. An analogous strategy combining exchangers with different lengths is shown in [67] for very deep BHEs (H > 600 m).

Fig. 2d shows the gain on total power (or heat extraction rates) by considering urban ground surface effects relative to the

undisturbed base case ($\Delta T_{GST}=0$). This is the increased technical geothermal potential associated with urban ground warming. For very low ΔT_{GST} , this gain is less than 5% while it could reach up to 30% depending on the time lag t_{urb} and the strength of ΔT_{GST} . As expected, the shallower the BHE is, the higher the relative gain in power. For a BHE with 200 m length, this gain for the studied depleting scenario ranges between 5% and 13%, even after 100 years of urban ground heating.

Menberg et al., Benz et al. and Zhu et al. [22,61,70] have studied the subsurface urban heat island phenomenon in several German cities. Zhu et al. [61] for instance, specifies for the city of Cologne magnitudes of ΔT_{GST} ranging between 2 and 4 K in build-up areas and more than 5 K in the city center. Taking into account that downtown cities are generally the oldest areas, the increased geothermal potential of a single BHE with H = 100 m could be between 10% and 25% higher than in less affected rural environments (Fig. 2d). Besides, its inherent spatial variability, ΔT_{CST} changes significantly with time. It is also influenced by multi-scale climate conditions, evolution in land use, surficial characteristics of pavements, and insulation of basements. The increased geothermal potential shown in Fig. 2d therefore represents an averaged firstorder estimation. Application to a specific site with temporally and spatially variable conditions is demonstrated later in Chapter 3.3.

The ratios depicted in Fig. 2d depend on the initial thermal conditions, minimum allowed fluid temperature and thermal diffusivity. Considering for instance a representative $\Delta T_{GST}=4$ K and H=100 m, the ratio is around 1.20. If the thermal diffusivity is between 50% and 200% of the reference value (Table 1), this ratio could vary between 1.21 and 1.26 for a low $T_k=8$ °C or between 1.16 and 1.21 for a high $T_k=12$ °C. This means that within the feasible ranges for diffusivities and non-affected GST in central European cities [70], the ratios in Fig. 2d are still robust estimates.

3.1.3. Renewable scenario

Given the conditions of the previous depleting scenario, the reservoir will be exhausted after 50 years of operation. Of similar interest are the conditions under which an unlimited exploitation in time can be achieved. The analysis is motivated by the response

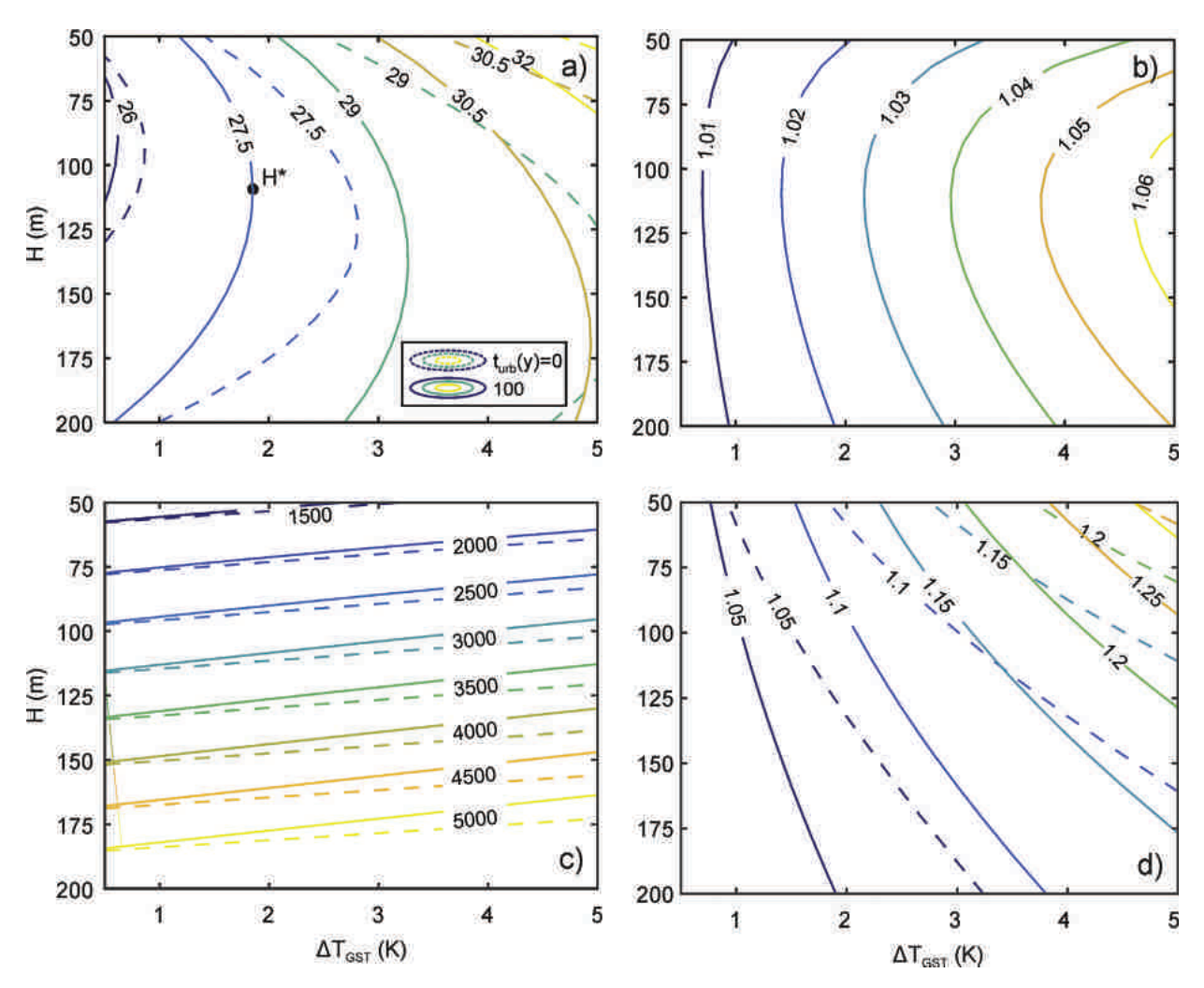


Fig. 2. Single BHE in the depleting scenario: a) heat extraction rates q (W m⁻¹), b) ratio q ($t_{urb} = 100$)/q ($t_{urb} = 0$) for the rates shown in a), c) extracted power (W), and d) ratio between the rates shown in a) and the ones from the base case (excluding the urban effect). Exemplarily, H^* is the length that requires the maximum ΔT_{GST} keeping q = 27.5 W m⁻¹.

of $\overline{T_{BW}}$ to ground surface temperature effects characterized in Fig. 1. Taking for example the curve with $Q_T=0$, which corresponds to the original g-function that ignores urbanization, it is shown that a 'renewable operation' is feasible approximately for $\ln(t/t_s) > 2$. At these times, axial effects and heat input from the ground surface compensate the continuous drop in the mean borehole wall temperature as discussed in [57]. However, reaching this state would require an operation time longer than 260 years for the parameters of Table 1 with H=100 m.

As can be seen also in Fig. 1, for $Q_T>0$, i.e. when accounting for urbanization, a sustainable operation can be achieved from the time when $\overline{\theta_{BW}}$ gets minimal. This minimum is reached earlier depending on the strength of ΔT_{GST} relative to q (measured through the dimensionless number Q_T). Fig. 3a depicts how this minimum changes as a function of t_{urb} and Q_T . With the lowest $Q_T\approx 0$, the minimum is reached at $\ln(t/t_s)>2$ as discussed earlier. However, taking a realistic $\Delta T_{GST}=4$ K and q=20 W m $^{-1}$, we obtain $Q_T=0.5$. Then, for H=100 m, the minimum is reached after 32 years for $t_{urb}=100$ years ($\ln(t/t_s)\approx -0.1$) or even after 12 years if $t_{urb}=0$ years ($\ln(t/t_s)\approx -1.1$). The larger t_{urb} is, the longer ΔT_{GST} has been acting before the BHE. Thus, it takes longer for the line source to balance the positive thermal effect of ΔT_{GST} (see also Fig. 1b). However, when reaching the minimum $\overline{\theta_{BW}}$ faster, this means lower mean borehole temperatures.

During simulation, the minimum temperature $\overline{T_{fluid}}$ can be set to the SIA's temperature threshold, and the corresponding maximum possible extraction rates can be computed (Eq. (7)). In the following, these rates are called "renewable rates". The ratios of these rates relative to the renewable ones obtained from the base case ($\Delta T_{GST} = 0$ K) are shown in Fig. 4a. These ratios are very similar to the ones shown in Fig. 2d (depleting operation), especially for $t_{urb} = 100$ years with values between 1.05 and 1.30. Fig. 4a however suggests a lower sensitivity to H that can be inferred from the depicted gradient, particularly for longer BHEs. This means that for obtaining a similar ratio as in Fig. 2d, a lower ΔT_{GST} is needed under renewable conditions. Still, the absolute renewable heat extraction rates are generally lower compared to the depleting scenario. This is summarized in Table 2.

After reaching the minimum $\overline{T_{BW}}$, the effect of ΔT_{GST} is more relevant than the rate q, and the borehole wall temperature increases (Fig. 1). Theoretically, it would be possible to further increase the heat extraction rates (for example by increasing the heating demand associated to the specific geothermal system) so that $\overline{T_{BW}}$ is kept at the given temperature threshold from that time on. The resulting heat extraction rate would be constant in time until the minimum temperature threshold is reached and then the rate could be increased monotonically until it arrives at a maximum value (Fig. 3b). At this maximum, the transient effect of ΔT_{GST}

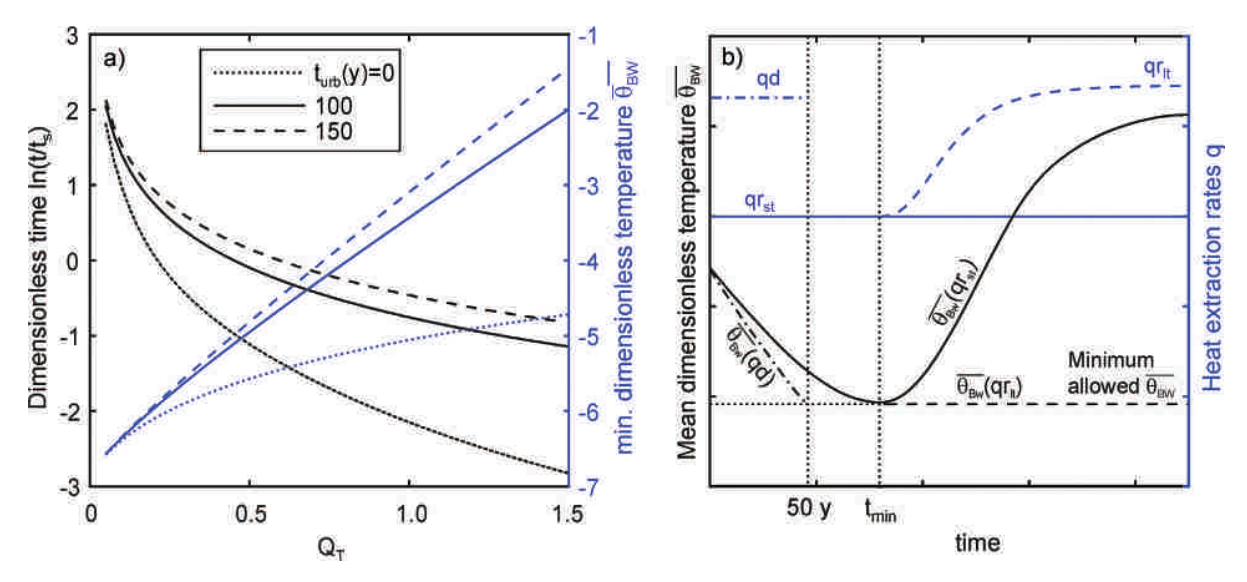


Fig. 3. a) Minimum dimensionless borehole temperature, min $(\overline{\theta_{BW}})$, and associated dimensionless time ln (t/t_s) , referential absolute magnitudes for time (years) and $\overline{T_{BW}}$ (°C) can be seen in Fig. 1b; b) schematic $(\overline{\theta_{BW}})$ (left axis) and corresponding heat extraction rates q (right axis) for the depleting (qd) and renewable (qr) scenarios. Rates qr are distinguished for the short term (qr_{st}) and for the long term (qr_{lt}) . $Q_T = \lambda \Delta T_{CST}/q$ and t_{urb} is the time lag (in years) between the start of BHE operation and the pre-existing ΔT_{CST} effect.

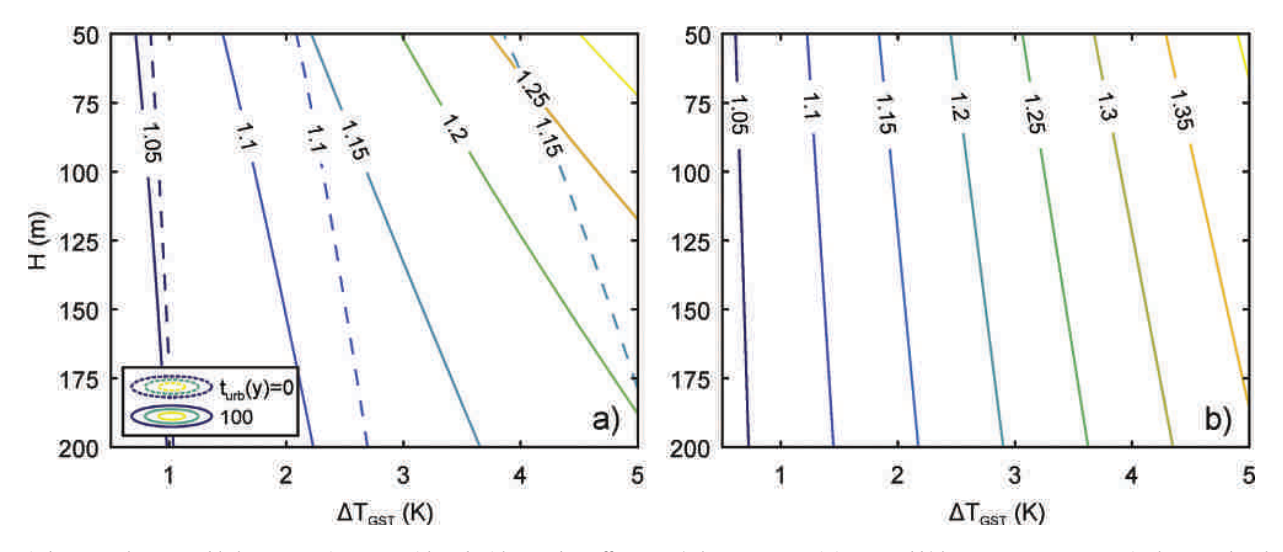


Fig. 4. Ratio between the renewable heat extraction rates with and without urban effects at: a) short-term or minimum and b) long-term or asymptote in the mean borehole wall temperature.

Table 2 Heat extraction rates (W m⁻¹) for a single ($B = \infty$) and a representative BHE in an infinite field for different degrees of urbanization and exploitation schemes, and $t_{urb} = 100$ years. R: renewable scenario, D: depleting scenario.

H (m)	B (m)	Base case		Low develo	opment	Suburban		Urban	
		$\Delta T_{GST} = 0 \text{ K}$		$\Delta T_{GST} = 1 \text{ K}$		$\Delta T_{GST} = 3 \text{ K}$		$\Delta T_{GST} = 5 \text{ K}$	
		R	D	R	D	R	D	R	D
50	10	3.9	5.8	4.2	6.2	4.8	6.9	5.5	7.7
	20	10.6	14.7	11.4	15.6	13.1	17.6	14.8	19.4
	30	16.0	20.0	17.3	21.3	19.8	23.9	22.4	26.5
	00	25.4	25.5	27.2	27.2	30.5	30.5	33.9	33.9
100	10	1.4	3.3	1.5	3.5	1.7	3.8	1.9	4.1
	20	4.1	10.1	4.4	10.6	5.0	11.6	5.6	12.6
	30	7.5	15.9	8.1	16.7	9.2	18.2	10.3	19.8
	00	24.7	25.3	26.2	26.5	28.8	28.9	31.3	31.3
200	10	0.6	2.8	0.6	2.8	0.7	3.0	0.7	3.1
	20	1.5	8.9	1.6	9.2	1.8	9.6	2.0	10.1
	30	2.9	14.9	3.1	15.3	3.4	16.1	3.8	16.9
	00	25.4	27.1	26.7	27.8	28.7	29.2	30.4	30.6

disappears, a new thermal equilibrium in the ground is reached and $\overline{\theta_{BW}}$ becomes again identical to the original g-function with $Q_T=0$. The initial thermal conditions however are now defined by the geothermal gradient and a new equilibrated ground surface temperature, which is the superposition of ΔT_{GST} and T_k .

Fig. 4b presents the ratios between the long-term maximum rates and the base case. By comparing Figs. 2d and 4b, it is shown that in the long-term renewable rates are between 5% and 10% higher than those calculated in the depleting scenario with prescribed life time of 50 years.

3.2. Infinite BHE field

Previous analysis reveals the consequence of urban ground heating for single BHE performance, but on the city scale, the concerted use of multiple BHEs has to be accounted for [7,9,71]. In such configurations or fields, the interaction and competition among BHEs may reduce the extractable heat per BHE when compared with a single installation [72]. For estimating the full urban technical geothermal potential, we therefore consider an extreme case, which is an infinite BHE field with borehole spacing B (squared lattice) and length H. This field mimics the idealistic behavior of a non-optimized large scale exploitation in a city, where all BHEs are similarly operated. These conditions facilitate the simulation through superimposed line sources, which invoke the linearity of the heat transport equation with known or constrained heat extraction rates at the borehole wall [33,37,73]. Following analysis continues using the parameters of the reference site listed in Table 1.

3.2.1. Depleting scenario

In the first step, the depleting scenario again considers mean fluid temperatures above $-1.5\,^{\circ}\text{C}$ during 50 years of operation. Fig. 5 depicts the energy densities in kWh per square meter and per year as a function of borehole length or installation depth H, and spacing B. The effect of long-term urbanization prior to BHE installation is included by assuming $t_{urb}=100\,$ years. Fig. 5a represents conditions of low ground heating of $\Delta T_{GST}=1\,$ K, which could be found for example beneath green spaces [22]. In comparison, a stronger ground heating of $\Delta T_{GST}=5\,$ K is depicted in Fig. 5b. As expected, in both figures, the highest energy densities are obtained for the deepest and more packed configurations.

For a separation of 30 m between standalone installations, for

instance, Fig. 5b gives energy densities between 13 and 33 kWh m⁻² a⁻¹ depending on the field depth. Taking the referential heating energy demands specified in Schiel et al. [7] for city buildings (between 102.3 and 207.1 kWh m⁻² a⁻¹), this would imply that for H = 200 m, the shallow ground could supply between 32% (33/102.3) and 16% (33/207.1) of these energy requirements for 50 years.

In this depleting scenario where the calculation time is fixed ($t=t_{urb}+50$ years), the ratio between energy densities, affected and unaffected (base case) by ΔT_{GST} , is independent of the separation B. Thus, the estimated increased technical geothermal potential computed for single BHE installations (Fig. 2b, d) is also valid for the infinite field.

3.2.2. Renewable scenario

Renewable use refers to heat extraction that does not only guarantee regulatory limits (here minimum of $-1.5\,^{\circ}\text{C}$ for heat carrier fluid) for a given time (here 50 years), but also beyond. As shown for single BHE operation (Chapter 3.1.3), continued reservoir depletion is associated with advancing replenishment, and ultimately ground heat flux can stimulate thermal recovery.

For a BHE in a field, the corresponding mean borehole wall temperature $\overline{\theta_{BW}}$ behaves similarly to the one shown in Fig. 1a for a single BHE and $Q_T=0$, but with lower magnitudes due to the interference with neighboring BHEs. The time for reaching renewable operation conditions in the base case (i.e., the curve's plateau) is also higher since influences from distant BHEs extend the transient behavior.

The effect of including an increased ground surface temperature is shown in Fig. 6. The energy densities are lower and clearly different from those in Fig. 5 (depleting scenario). In the latter, the highest energy density is obtained with a deeper field, while in the renewable scenario, the shallowest field is favored. This is due to the unconstrained exploitation time under renewable conditions. To fulfil this, the system is forced to take more heat from increased GST rather than depleting the reservoir. In both exploitation schemes the maximum in energy densities are obtained for the most packed fields.

Fig. 6a depicts the case of $\Delta T_{CST} = 1$ K with minor heat flux. The ratio between these densities and those from the base case ($\Delta T_{CST} = 0$ K) is depicted in Fig. 6c, and urbanization here yields up to 8% higher densities, and consequently, extraction rates. An increased ground surface temperature of 1 K might be associated

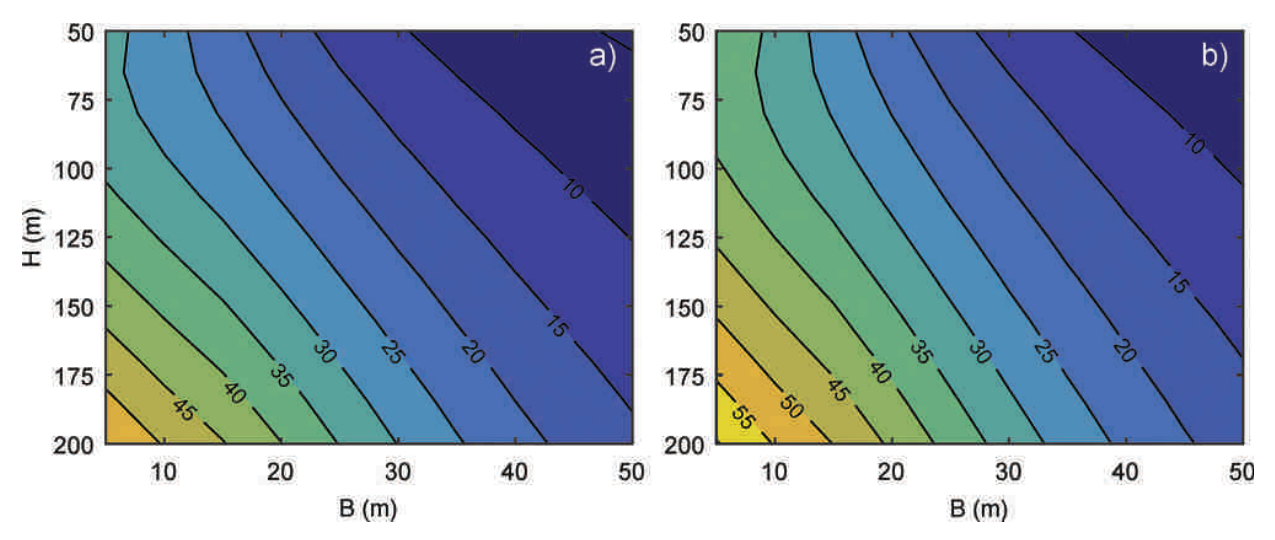


Fig. 5. Energy densities (kWh m⁻² a⁻¹) for the infinite field with $t_{urb}=100$ years under the depleting scenario: a) $\Delta T_{CST}=1$ K and b) $\Delta T_{GST}=5$ K.

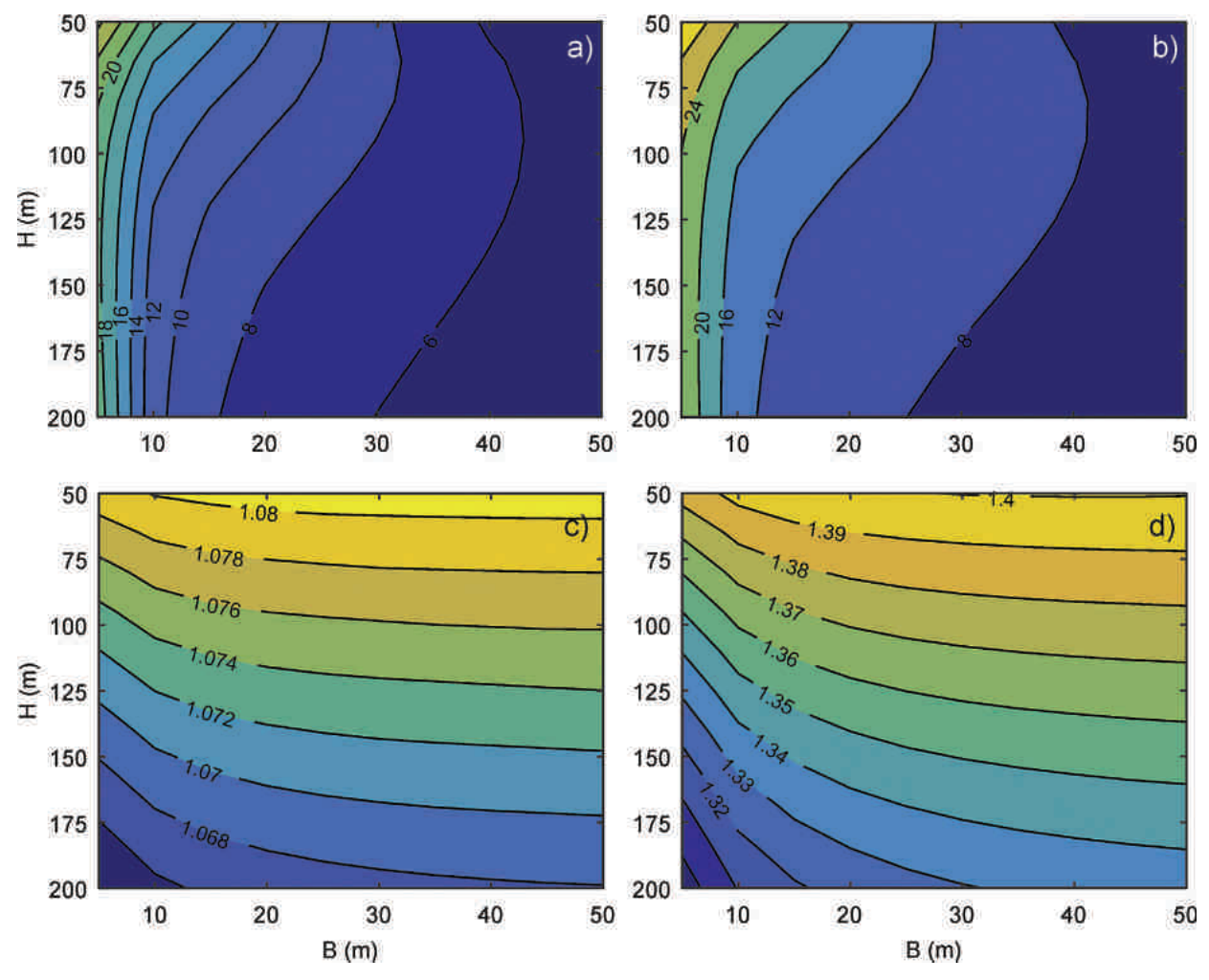


Fig. 6. Energy densities (kWh m⁻² a⁻¹): a) $\Delta T_{GST} = 1$ K, b) $\Delta T_{GST} = 5$ K, c) ratio of renewable rates with $\Delta T_{GST} = 1$ K with respect to the renewable base case and d) ratio of renewable rates with $\Delta T_{GST} = 5$ K with respect to the renewable base case.

with a loose and open development in suburban areas. Taking again the energy heating demands specified in [7] for this type of settlement (57.7 kWh m $^{-2}$ a $^{-1}$), the results indicate that it would be possible to supply between 14% and 17% of this demand in a renewable way. To accomplish this, BHEs of around 100 m long are required with a separation between 20 and 30 m.

Fig. 6b depicts the other extreme: renewable energy densities for $\Delta T_{CST} = 5$ K, such as is common in many city centers. By relating to the densities in the base case, Fig. 6d indicates that the renewable rates in the city center would be between around 30%–40% higher than outside the city.

From the comparison with the depleting densities shown in Fig. 5b, it can be concluded that the latter are between 25% and 65% higher. The value of 25% refers to the most shallow and packed fields, and 65% to the deepest and more spread fields. A related analysis is presented in Table 2 in terms of absolute heat extraction rates (W m $^{-1}$) for both exploitation scenarios and different system configurations. In general, for single BHEs the SIA's requirements seem to be a good guideline to ensure renewability since discrepancies to the depleting scenario are not significant. For the infinite field however, the situation is different especially for longer systems. Under non-urbanized conditions ('Base case' in Table 2) for example, depleting rates could be about six times higher than the renewable ones (H = 200 m and B = 20 m). This difference declines with shallower systems and stronger urban effect (ΔT_{GST}) reaching

values between 1.19 and 1.40 for H = 50 m and $\Delta T_{GST} = 5$ K.

Finally, it is interesting to compare the energy densities of Fig. 6b with the corresponding heating energy demand in urban settlements (between 102.3 and 207.1 kWh m⁻² a⁻¹) [7]. For the most optimistic scenario (B < 10 m, H < 60 m), it would be possible to supply 13–27% (in a renewable way) of the heating demand associated with settlements, such as downtown city buildings. For more realistic BHE separation of B = 20-30 m, this percentage would be only between 6% and 16%. These numbers of course are restricted to the parameters of the presented case study (Table 1).

3.3. Case study

This case study aims at demonstrating the applicability of the methodology at a real site with specific (time dependent) land use distribution. It does not only include the effect of elevated heat flux from urban structures, but also atmospheric warming due to long-term climate change. The site is located in the suburb of Meilen in the city of Zurich (Fig. 7a), where a temperature-depth profile (TDP) was measured prior to BHE operation (Bayer et al. [21]). For this site, Fig. 7b shows the most influential urban structures that can be classified as buildings (B) or pavements (A). Most of the buildings were built within the period between 1959 and 1972. However, three on the west side (B17–B19) date back to 1884. The streets are also rather old with an age of more than 100 years.

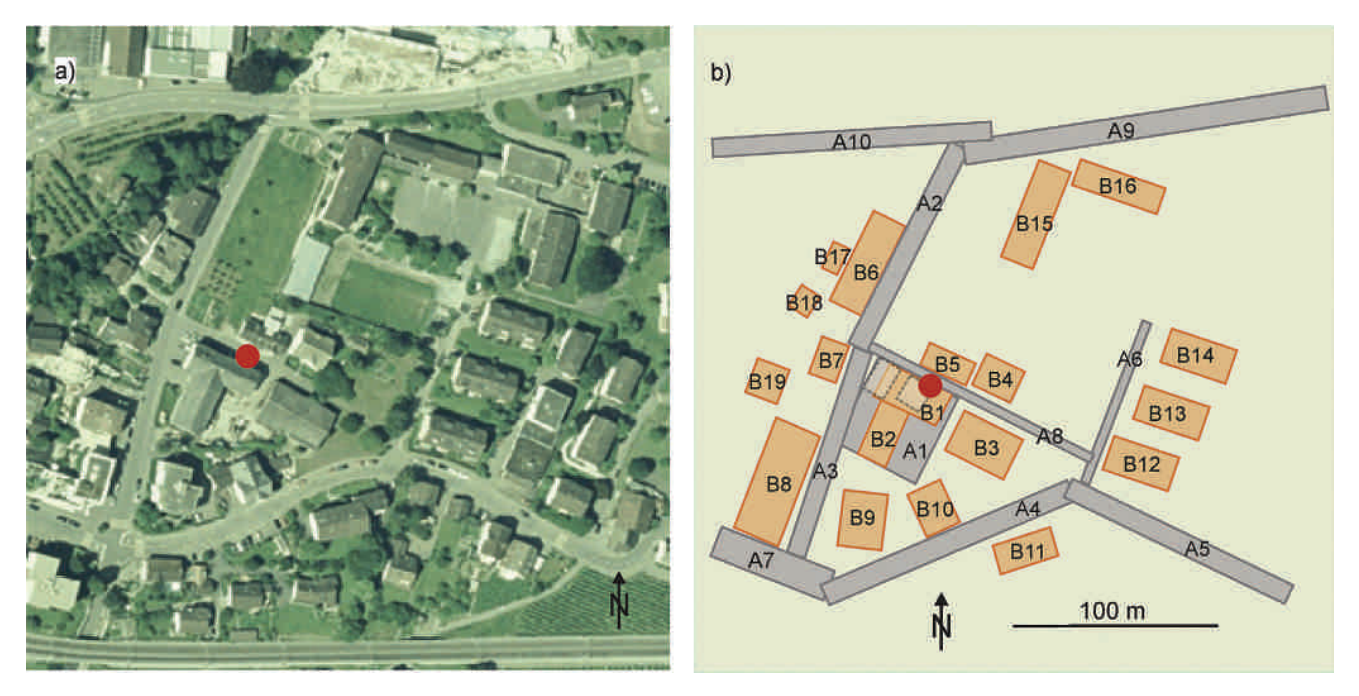


Fig. 7. a) Plan view of the site as of 2005 [74] and b) influencing buildings (B) and pavements (A). The lighter orange areas surrounded by dashed lines represent buildings demolished in 1959, whose thermal influence is included in the simulation. The red point indicates the BHE location (more details in Bayer et al. [21]). (For interpretation of the references to colour in this figure legend, the reader is referred to the web version of this article.)

By superposing non-homogeneous solutions for the conductive-dominated problem, Bayer et al. [21] reproduced the measured TDP (Fig. 8a). Their procedure was based in a stochastic inversion that yielded estimations of the ground surface temperature of pavements and buildings. Their methodology was also capable of differentiating between the thermal influences due to climate forcing and the identified urban structures.

For the estimation of the increased technical potential, this work

considers a BHE installed at the measuring point starting operation in 2005 (same year as the measurement). The mean temperature at the borehole wall is obtained by superposing Eq. (4) (for each urban structure) to the background effect representing undisturbed green space. According to Bayer et al. [21], the ground surface temperature for green open spaces and pavements is a function of the surface air temperature (SAT). The latter has been known for the last 130 years with a daily resolution. However, it is necessary to fit

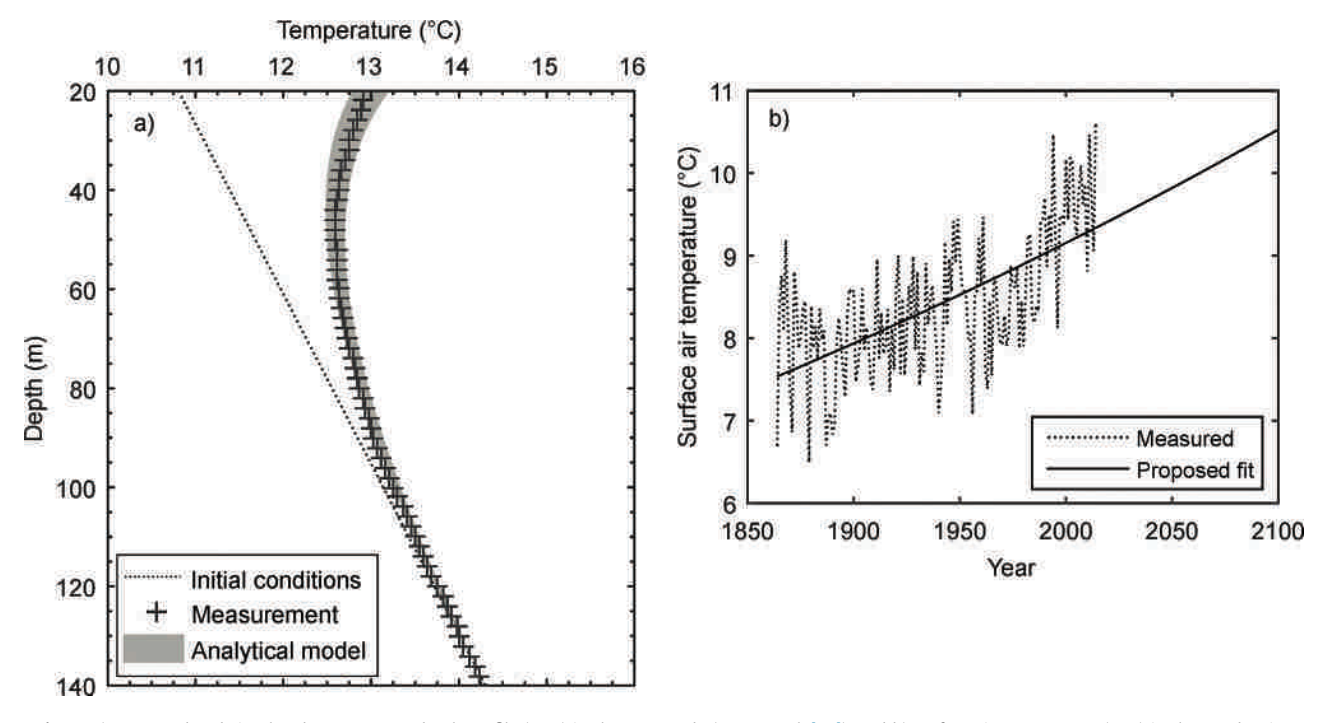


Fig. 8. a) Measured and simulated temperature-depth profile (TDP) in the case study (Bayer et al. [21]), and b) surface air temperature (SAT) in the nearby site.

an analytical expression in order to extrapolate SAT during the operation time (2005 onwards). The fit curve is shown in Fig. 8b and follows a logistic model with a maximum of 10.5 °C in 2100.

For different borehole lengths, Fig. 9a depicts the extractable mean annual heat extraction rates under depleting conditions $(\overline{T_{fluid}} = -1.5^{\circ}C)$ after 50 years). Fig. 9a distinguishes two different cases on its left axis: base case without increased ground surface effects (N) and the total effect including urban structures (N + U). On the right axis of Fig. 9a, the rate ratio (N + U)/N is indicated. For H = 100 m for example, the total increased GST effect (N + U) allows to extract up to 18% more energy than in the base case (N).

Fig. 9b shows the ratios between renewable and depleting rates (left axis), as well as the times to reach renewability (right axis). The results indicate that there are not significant differences between the exploitation schemes. This is a consequence of installing a single BHE in an environment with pre-existing warming and agrees with the previous discussion on renewability for single BHEs (Chapter 3.1.3 and Table 2). According to Fig. 9b, with a BHE of around 145 m length, given the SIA requirements, renewable operation after 50 years is feasible.

4. Summary and conclusions

This study addresses two major aspects when operating borehole heat exchangers (BHEs) in urban environments. First, it is revealed that the technical geothermal potential of utilizing urban ground can be substantially higher (up to 40%) than in rural, open green spaces. This is due to urban ground warming, caused by heat loss and accelerated heat flux from urban structures, which are characteristic for many cities worldwide. Second, it is demonstrated how urban ground warming enhances the renewal of BHEs operated in unbalanced way. For this, ground energy exploitation, within a given time to a given temperature threshold, is compared to long-term renewable operation.

A summary of the increased technical potential when comparing feasible heat extraction rates in cities to those in the rural surrounding is provided in Table 3. These values are obtained by taking the ratio of heat extraction rates under different degrees of urbanization divided by the corresponding ones of the non-perturbed base case as listed in Table 2. The increased technical potential is clearly dominated by the relative ground heating, ΔT_{GST} .

Table 3 Increased technical geothermal potential for single $(B=\infty)$ and the representative BHE in an infinite field for different degrees of urbanization and exploitation schemes and $t_{urb}=100$ years. R: renewable scenario, D: depleting scenario.

H (m)	B (m)	Low development $\Delta T_{GST} = 1 \text{ K}$		Suburban		Urban	
				$\Delta T_{GST} =$	$\Delta T_{GST} = 3 \text{ K}$		$\Delta T_{GST} = 5 \text{ K}$
		R	D	R	D	R	D
50	10	1.08	1.07	1.24	1.20	1.40	1.33
	20	1.08		1.24		1.40	
	30	1.08		1.24		1.40	
	00	1.07		1.20		1.33	
100	10	1.08	1.05	1.22	1.14	1.37	1.24
	20	1.08		1.22		1.37	
	30	1.08		1.22		1.37	
	00	1.06		1.17		1.27	
200	10	1.07	1.03	1.20	1.08	1.30	1.13
	20	1.07		1.20		1.32	
	30	1.07		1.20		1.33	
	00	1.05		1.13		1.19	

while borehole length H and separation B have a secondary role. As expected, the increased potentials are higher for shallower systems. For highly urbanized conditions ($\Delta T_{GST} = 5$ K), full exploitation rates increase by 13–33%, and renewable rates by even 19–40%. However, note that the absolute renewable rates are generally lower (Table 2). In essence, this means that either higher energy extraction is feasible in urban ground, or the borehole length can be reduced. As a rough estimate, each additional degree of ground heating saves 4 borehole meters.

Table 4 summarizes, what share of the urban heating energy demand (according to [7]) can be covered by operating BHEs in an infinite field. In (sub)urban areas, 4–16% of the heating demand could be supplied in a renewable way. Apparently, towards the city center the energy demand grows more than the stored geothermal energy. Since replenishment comes mainly from the ground surface, here shallower systems are favorable. However, when full reservoir exploitation is considered, values of up to 40% can be achieved by deep boreholes of up to 200 m. Not only the accessed ground volume but also the ground heat flux may be decisive for the appropriate borehole depth and configuration. As another example, consider depleting exploitation of warmed urban ground ($\Delta T_{GST} = 5$ K). Here, the extractable energy is similar for H = 50 m

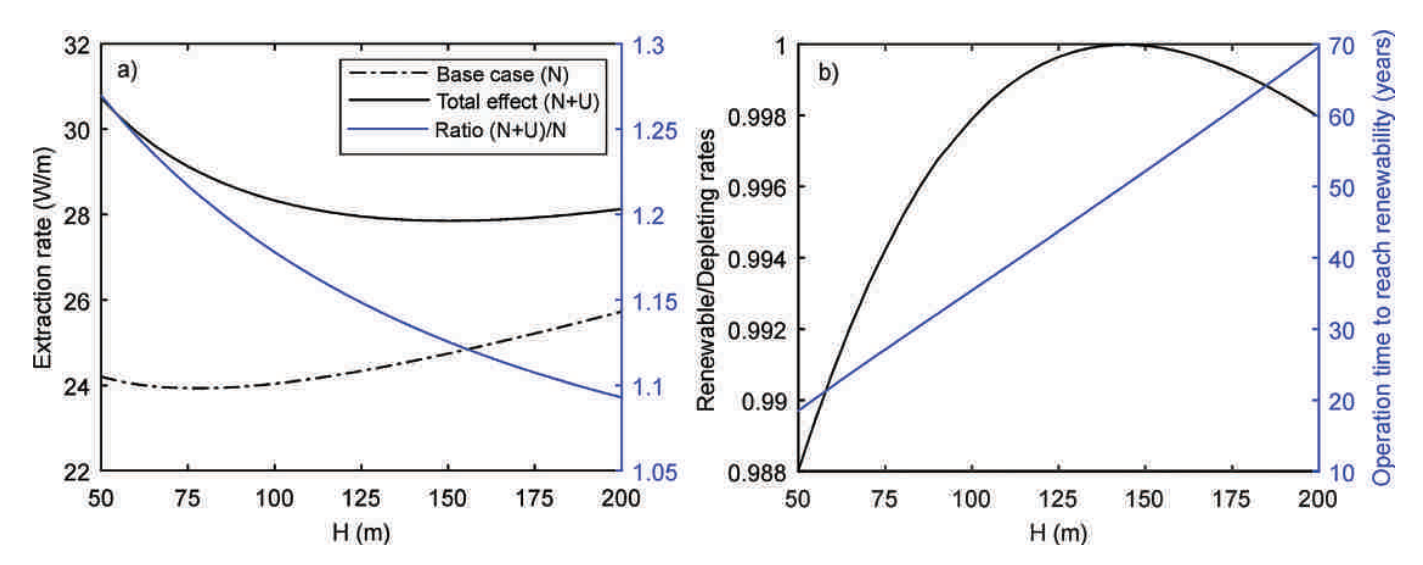


Fig. 9. a) Depleting heat extraction rates in the case study for different scenarios: base case (N) and total GST effect (N + U); b) ratio renewable/depleting rates (left axis) and time to reach short term renewability (right axis).

Table 4 Share of the heating demand supplied by an infinite BHE field for different degrees of urbanization and exploitation schemes and $t_{urb} = 100$ years. The considered heating demands (in kWh m⁻² a⁻¹) are as follows [7]: 60 for low development areas, 130 for suburban areas and 170 for city centers. R: renewable scenario, D: depleting scenario.

H (m)	B (m)	$\frac{\text{Low}}{\text{development}}$ $\frac{\Delta T_{GST} = 1 \text{ K}}{\text{ K}}$		Suburban $\Delta T_{GST} = 3 \text{ K}$		City center $\Delta T_{GST} = 5 \text{ K}$	
		R	D	R	D	R	D
50	10	32%	47%	16%	23%	14%	20%
	20	22%	30%	11%	15%	10%	12%
	30	15%	18%	7%	9%	6%	8%
100	10	22%	53%	11%	26%	10%	21%
	20	17%	40%	8%	19%	7%	16%
	30	14%	28%	7%	14%	6%	11%
200	10	18%	86%	9%	40%	8%	32%
	20	12%	69%	6%	32%	5%	26%
	30	10%	52%	5%	24%	4%	19%

and 100 m, as reflected by the similar shares of around 20% listed in Table 4 (B=10 m). This is a consequence of the competing effect between accelerated ground heat flux and the geothermal gradient. Considering the highest magnitudes of ΔT_{GST} with $t_{urb}=100$ years, installing a BHE field with H=100 m is not likely the best strategy, since almost the same power can be extracted with a shallower system that takes advantage of the cumulated urban heat. However, for longer BHE fields (H=200 m) the geothermal gradient dominates and the energy yield is enhanced.

The findings presented here are crucial for planning geothermal systems in regions with elevated ground temperatures. Such subsurface urban heat islands, however are not only caused by heat loss from basements and accelerated heat flux through paved ground. In cities, there exist several additional sources such as sewage channels, district heating systems or tunnels. Aside from this, long-term atmospheric warming has to be accounted for. All these factors countervail ground cooling from geothermal energy use, and thus facilitate renewable operation without active replenishment. Strictly speaking, however, we do not tap a naturally renewable energy source. In a nutshell, shallow geothermal systems recycle urban ground heat losses.

Acknowledgements

This work was supported by the Swiss National Science Foundation (SNSF) under grant number 200021L 144288, and the German Research Foundation (DFG), under grant number BL 1015/4-1. We thank Rachael Colldeweih for language corrections.

References

- [1] J.W. Lund, T.L. Boyd, Direct utilization of geothermal energy 2015 worldwide review, Geothermics 60 (2016) 66–93.
- [2] S. Bauer, et al., Impacts of the use of the geological subsurface for energy storage: an investigation concept, Environ. earth Sci. 70 (8) (2013) 3935–3943.
- [3] S. Hähnlein, et al., Sustainability and policy for the thermal use of shallow geothermal energy, Energy Policy 59 (2013) 914–925.
- [4] M. Alcaraz, et al., Use rights markets for shallow geothermal energy management, Appl. Energy 172 (2016) 34–46.
- [5] R. Wagner, T. Weisskopf, Erdsondenpotenzial in der Stadt Zürich, Im Auftrag des Amtes für Hochbauten der Stadt Zürich, 2014.
- [6] A. Gemelli, A. Mancini, S. Longhi, GIS-based energy-economic model of low temperature geothermal resources: a case study in the Italian Marche region, Renew. Energy 36 (9) (2011) 2474–2483.
- [7] K. Schiel, et al., GIS-based modelling of shallow geothermal energy potential for CO₂ emission mitigation in urban areas, Renew. Energy 86 (2016) 1023–1036
- [8] J. Ondreka, et al., GIS-supported mapping of shallow geothermal potential of

- representative areas in south-western Germany—possibilities and limitations, Renew. Energy 32 (13) (2007) 2186–2200.
- [9] Y. Zhang, K. Soga, R. Choudhary, Shallow geothermal energy application with GSHPs at city scale: study on the City of Westminster, Géotechnique Lett. 4 (April—June) (2014) 125—131.
- [10] A. Casasso, R. Sethi, Territorial analysis for the implementation of geothermal heat pumps in the province of Cuneo (NW Italy), Energy Procedia 78 (2015) 1159–1164.
- [11] F. Jaudin, et al., Thermomap-an open-source web mapping application for illustrating the very shallow geothermal potential in europe and selected case study areas, in: European Geothermal Congress 2013, EGC 2013, 2013.
- [12] M. Alcaraz, et al., Advection and dispersion heat transport mechanisms in the quantification of shallow geothermal resources and associated environmental impacts. Sci. Total Environ. 543 (Part A) (2016) 536–546.
- [13] VDI, Thermische Nutzung des Untergrundes (Guideline for thermal use of the underground), in: VDI-Richtlinie 4640, Verein Deutscher Ingenieure (VDI)-Gesellschaft Energietechnik, Germany, 2012.
- [14] Y. Zhang, R. Choudhary, K. Soga, Influence of GSHP system design parameters on the geothermal application capacity and electricity consumption at city-scale for Westminster, London, Energy Build. 106 (2015) 3–12.
- [15] S. Arthur, et al., Modelling large ground source cooling systems in the Chalk aquifer of central London, Q. J. Eng. Geol. Hydrogeol. 43 (3) (2010) 289–306.
- [16] K. Menberg, et al., Long-term evolution of anthropogenic heat fluxes into a subsurface urban heat island, Environ. Sci. Technol. 47 (17) (2013) 9747–9755
- [17] M. Taniguchi, T. Uemura, K. Jago-on, Combined effects of urbanization and global warming on subsurface temperature in four Asian cities, Vadose Zone J. 6 (3) (2007) 591–596.
- [18] A. Revesz, et al., Ground source heat pumps and their interactions with underground railway tunnels in an urban environment: a review, Appl. Therm. Eng. 93 (2016) 147–154.
- [19] Bidarmaghz, A., et al., The importance of surface air temperature fluctuations on long-term performance of vertical ground heat exchangers. Geomech. Energy Environ.
- [20] J. Eggleston, K.J. McCoy, Assessing the magnitude and timing of anthropogenic warming of a shallow aquifer: example from Virginia Beach, USA, Hydrogeol. J. (2014) 1–16.
- [21] P. Bayer, et al., Extracting past atmospheric warming and urban heating effects from borehole temperature profiles, Geothermics 64 (2016) 289–299.
- [22] S. Benz, et al., Spatial resolution of anthropogenic heat fluxes into urban aquifers, Sci. Total Environ. 524–525 (0) (2015) 427–439.
- [23] N. Müller, W. Kuttler, A.-B. Barlag, Analysis of the subsurface urban heat island in Oberhausen, Germany, Clim. Res. 58 (3) (2014) 247–256.
- [24] Z. Luo, C. Asproudi, Subsurface urban heat island and its effects on horizontal ground-source heat pump potential under climate change, Appl. Therm. Eng. 90 (2015) 530–537.
- [25] K. Zhu, et al., The geothermal potential of urban heat islands, Environ. Res. Lett. 5 (4) (2010) 044002.
- [26] L. Rybach, Classification of geothermal resources by potential, Geotherm. Energy Sci. 3 (2015) 13–17.
- [27] C. Yavuzturk, Modeling of Vertical Ground Loop Heat Exchangers for Ground Source Heat Pump Systems, Oklahoma State University, 1999.
- [28] P. Hein, et al., A numerical study on the sustainability and efficiency of borehole heat exchanger coupled ground source heat pump systems, Appl. Therm. Eng. 100 (2016) 421–433.
- [29] N. Aranzabal, et al., Extraction of thermal characteristics of surrounding geological layers of a geothermal heat exchanger by 3D numerical simulations, Appl. Therm. Eng. 99 (2016) 92–102.
- [30] R. Perego, et al., Sustainability evaluation of a medium scale GSHP system in a layered alluvial setting using 3D modeling suite, Geothermics 59 (Part A) (2016) 14–26.
- [31] P. Eskilson, Thermal analysis of Heat Extraction Boreholes, Ph.D. Thesis, University of Lund, Lund, Sweden, 1987.
- [32] M. Li, A.C.K. Lai, Review of analytical models for heat transfer by vertical ground heat exchangers (GHEs): a perspective of time and space scales, Appl. Energy 151 (0) (2015) 178–191.
- [33] J. Claesson, S. Javed, An analytical method to calculate borehole fluid temperatures for time-scales from minutes to decades, ASHRAE Trans. 117 (2) (2011) 279–288.
- [34] J. Wei, et al., A new analytical model for short-time response of vertical ground heat exchangers using equivalent diameter method, Energy Build. 119 (2016) 13–19.
- [35] A. Lazzarotto, A network-based methodology for the simulation of borehole heat storage systems, Renew. Energy 62 (2014) 265–275.
- [36] M. Cimmino, M. Bernier, F. Adams, A contribution towards the determination of g-functions using the finite line source, Appl. Therm. Eng. 51 (1) (2013) 401–412.
- [37] L. Lamarche, B. Beauchamp, A new contribution to the finite line-source model for geothermal boreholes, Energy Build. 39 (2) (2007) 188–198.
- [38] T. Bandos, et al., Finite line-source model for borehole heat exchangers: effect of vertical temperature variations, Geothermics 38 (2) (2009) 263–270.
- [39] H. Zeng, N. Diao, Z. Fang, A finite line-source model for boreholes in geothermal heat exchangers, Heat Transfer—Asian Res. 31 (7) (2002) 558–567.
- [40] A. Lazzarotto, A Methodology for the Calculation of Response Functions for

- Geothermal Fields with Arbitrarily Oriented Boreholes: Part 1, 2015.
- [41] S. Erol, M.A. Hashemi, B. François, Analytical solution of discontinuous heat extraction for sustainability and recovery aspects of borehole heat exchangers, Int. J. Therm. Sci. 88 (2015) 47–58.
- [42] M. Cimmino, M. Bernier, A semi-analytical method to generate g-functions for geothermal bore fields, Int. J. Heat Mass Transf. 70 (2014) 641–650.
- [43] A. Lazzarotto, F. Björk, A methodology for the calculation of response functions for geothermal fields with arbitrarily oriented boreholes—Part 2, Renew. Energy 86 (2016) 1353—1361.
- [44] J.A. Rivera, P. Blum, P. Bayer, Analytical simulation of groundwater flow and land surface effects on thermal plumes of borehole heat exchangers, Appl. Energy 146 (0) (2015) 421–433.
- [45] J.A. Rivera, P. Blum, P. Bayer, Influence of spatially variable ground heat flux on geothermal systems: line source model with nonhomogeneous Cauchy-type top boundary conditions, Appl. Energy (2016) (Accepted).
- [46] H. Carslaw, J. Jaeger, Conduction of Heat in Solids, second ed., Oxford University Press, , New York, 1959.
- [47] M.N. Özışık, Boundary Value Problems of Heat Conduction, Courier Corporation, 1989.
- [48] X. Duan, G.F. Naterer, Ground heat transfer from a varying line source with seasonal temperature fluctuations, J. Heat. Transf. 130 (11) (2008), 111302—111302.
- [49] J. Claesson, P. Eskilson, Conductive heat extraction to a deep borehole: thermal analyses and dimensioning rules, Energy 13 (6) (1988) 509–527.
- [50] P. Bayer, et al., Extracting past atmospheric warming and urban heating effects from borehole temperature profiles, Geothermics 64 (2016) 289–299.
- [51] J.A. Rivera, P. Blum, P. Bayer, Influence of spatially variable ground heat flux on closed-loop geothermal systems: line source model with nonhomogeneous Cauchy-type top boundary conditions, Appl. Energy 180 (2016) 572–585.
- [52] C.A. Taylor, H.G. Stefan, Shallow groundwater temperature response to climate change and urbanization, J. Hydrol. 375 (3) (2009) 601–612.
- [53] J.C. Choi, J. Park, S.-R. Lee, Numerical evaluation of the effects of groundwater flow on borehole heat exchanger arrays, Renew. Energy 52 (2013) 230–240.
- [54] A. Angelotti, et al., Energy performance and thermal impact of a Borehole Heat Exchanger in a sandy aquifer: influence of the groundwater velocity, Energy Convers. Manag. 77 (2014) 700–708.
- [55] C.-E. Hagentoft, Heat losses and temperature in the ground under a building with and without ground water flow—II. Finite ground water flow rate, Build. Environ, 31 (1) (1996) 13–19.
- [56] N. Molina-Giraldo, et al., A moving finite line source model to simulate borehole heat exchangers with groundwater advection, Int. J. Therm. Sci. 50 (12) (2011) 2506–2513.
- [57] J.A. Rivera, P. Blum, P. Bayer, Ground energy balance for borehole heat exchangers: vertical fluxes, groundwater and storage, Renew. Energy 83 (0)

- (2015) 1341-1351.
- [58] A. García-Gil, et al., GIS-supported mapping of low-temperature geothermal potential taking groundwater flow into account, Renew. Energy 77 (2015) 268–278.
- [59] J. Epting, F. Händel, P. Huggenberger, Thermal management of an unconsolidated shallow urban groundwater body, Hydrology Earth Syst. Sci. 17 (5) (2013) 1851–1869.
- [60] A. García-Gil, et al., The thermal consequences of river-level variations in an urban groundwater body highly affected by groundwater heat pumps, Sci. Total Environ. 485–486 (0) (2014) 575–587.
- [61] K. Zhu, et al., Groundwater temperature evolution in the subsurface urban heat island of Cologne, Germany, Hydrol. Process. 29 (6) (2015) 965–978.
- [62] G. Attard, et al., Deterministic modeling of the impact of underground structures on urban groundwater temperature, Sci. Total Environ. 572 (2016) 986–994.
- [63] S. Haehnlein, P. Bayer, P. Blum, International legal status of the use of shallow geothermal energy, Renew. Sustain. Energy Rev. 14 (9) (2010) 2611–2625.
- [64] SIA:384/6, Erdwärmesonden, Schweizerischer Ingenieur- und Architektenverein, Zürich, 2010.
- [65] P. Ungemach, M. Papachristou, M. Antics, Renewability versus sustainability. A reservoir management approach, in: Proceedings of the European Geothermal Congress, 2007.
- [66] F. Stauffer, et al., Thermal use of Shallow Groundwater, CRC Press, 2013.
- [67] H. Holmberg, et al., Deep borehole heat exchangers, application to ground source heat pump systems, in: Submitted to the World Geothermal Congress, 2015
- [68] L. Rybach, W. Eugster, Sustainability aspects of geothermal heat pump operation, with experience from Switzerland, Geothermics 39 (4) (2010) 365–369.
- [69] S.P. Kavanaugh, K.D. Rafferty, Ground-source Heat Pumps: Design of Geothermal Systems for Commercial and Institutional Buildings, American Society of Heating, Refrigerating and Air-Conditioning Engineers, 1997.
- [70] K. Menberg, et al., Subsurface urban heat islands in German cities, Sci. Total Environ. 442 (2013) 123–133.
- [71] J. Allegrini, et al., A review of modelling approaches and tools for the simulation of district-scale energy systems, Renew. Sustain. Energy Rev. 52 (2015) 1391–1404.
- [72] P. Eskilson, J. Claesson, Simulation model for thermally interacting heat extraction boreholes, Numer. Heat. Transf. 13 (2) (1988) 149–165.
- [73] P. Bayer, M. de Paly, M. Beck, Strategic optimization of borehole heat exchanger field for seasonal geothermal heating and cooling, Appl. Energy 136 (2014) 445–453.
- [74] ARG, Orthofoto SWISSIMAGE 2002 Perimeter des Kantons Zürich, Amt für Raumentwicklung Geoinformation, Zürich, 2002.